Effect of Drying Temperatures and Diffusion Path Lengths on Effective Moisture Diffusivity and Activation Energy of Red Delicious Apple Slices Under Convective Drying

Oldřich Dajbych , Abraham Kabutey * , Čestmír Mizera , Aleš Sedláček , David Herak

Posted Date: 10 February 2026

doi: 10.20944/preprints202602.0791.v1

Keywords: drying kinetics; Fickian second law; Arrhenius model; moisture transport; diffusion behaviour

 doi:10.20944/preprints202602.0791.v1

Article

Effect of Drying Temperatures and Diffusion Path Lengths on Effective Moisture Diffusivity and Activation Energy of Red Delicious Apple Slices Under Convective Drying

Oldřich Dajbych, Abraham Kabutey *, Čestmír Mizera, Aleš Sedláček and David Herak

Department of Mechanical Engineering, Faculty of Engineering, Czech University of Life Sciences Prague, 165 20 Prague, Czech Republic

* Correspondence: kabutey@tf.czu.cz; Tel.: +420-22438-3180

Abstract

Modelling of the food drying process is dependent on the understanding of the complex moisture transport mechanisms. This study analyzed the effect of drying temperatures ranging from 40 to 80 °C and diffusion path lengths (initial, average and final half-thicknesses) on the shrinkage, effective moisture diffusivity and activation energy of thin-layer red delicious apple samples under convective drying. Fick's second law and Arrhenius model were utilized to determine the effective moisture diffusivity and activation energy. The mean shrinkage increased from 31.09% at 40 °C to a maximum of 42.65% at 70, then slightly decreased to 36.77% at 80 °C, indicating that shrinkage does not increase linearly with drying temperature. The initial, average and final half-thicknesses yielded effective moisture diffusivities ranging from 1.43×10^{-10} m²/s to 1.03×10^{-09} m²/s, with the average dimension providing the most realistic representation of the effective moisture diffusion path during drying. The linear regression models between the natural logarithm of the moisture ratio and drying time showed a strong fit with R^2 values ranging from 0.9955 to 0.9971, confirming the reliability of Fick's second law for describing the effective moisture diffusivity. The mean activation energy ranged from 21.56 to 26.03 kJ/mol across the different characteristic lengths, indicating the minimum energy requirement for moisture diffusion in red delicious apple samples during the convective drying.

Keywords: drying kinetics; Fickian second law; Arrhenius model; moisture transport; diffusion behaviour

1. Introduction

Apples are among the fruits and vegetables that have a high moisture content, ranging from 80 to 95% on a wet basis. They are classified as highly perishable commodities or susceptible to microbial infection and spoilage during storage [1–4]. Drying can reduce the moisture content and extend the shelf life of fruits and vegetables [1,5,6]. Convective (hot-air oven) drying, microwave drying, infrared drying, and freeze drying are among the drying techniques; however, hot-air oven drying is the most used drying method [1,2,7,8].

Food drying is a complex process coupled with heat and moisture transfer [9–13]. Knowledge of the moisture transport process is essential for understanding and accurately modelling the food drying process [11,14,15]. Effective moisture diffusivity is a critical parameter for characterizing intrinsic moisture transfer mechanisms during the drying process [9–11,16]. It describes the mechanisms of moisture movement within the product, a key transport property applicable to the mathematical modelling of various food processes, including drying [9,10,16–18]. Fick's mathematical model explicitly correlates moisture diffusivity with drying rates, especially during the falling-rate drying stage [9–11,19,20]. Several studies have successfully applied the Fickian model to

 doi:10.20944/preprints202602.0791.v1

determine the average effective moisture diffusivities of different food materials using slope method, assuming constant moisture diffusivity throughout the drying process [9,11,18,19,21,22]. The influence of drying temperature is commonly studied using an Arrhenius-type relationship [9,11,21,23]. Studies have indicated that moisture and temperature could significantly influence moisture diffusivity in biological and food materials [9,17].

Recently, drying various fruit slices such as peach, apricot, apple, orange, kiwi, banana, is common, and dried products are sold at very high prices in the market [24]. In literature, several drying techniques and pretreatments have been adopted for drying different varieties of apple slices, with the aim of evaluating or describing the drying kinetics, colour change, quality attributes, microstructure, moisture diffusivity, activation energy, and energy and exergy analysis [1,2,9,10,25–31]. The development of energy-efficient, cost effective, and high-quality drying techniques has been a current research trend [9,26].

However, the results of our previously published work on red delicious apple slices dried using infrared and hot-air oven methods [27] showed that drying temperature and method influenced the drying behaviour and quality of the red delicious apple slices. Infrared (IR) drying consistently achieved faster moisture removal than hot-air oven (OV) drying at all temperatures (40–80 °C). Equilibrium moisture content was reached at drying temperatures above 50 °C, whereas 40 °C was insufficient within 10 h. Colour parameters exhibited non-linear trends with temperature at higher temperatures (60–80 °C). IR drying resulted in lower total colour change, chroma, colour index, and browning index than OV drying, indicating better colour preservation, whereas at lower temperatures (40–50 °C), IR caused greater colour changes. Rehydration ratio ranged from approximately 1.33 to 2.05 g/g and depended on both temperature and method, with IR drying generally promoting better rehydration due to reduced structural damage and higher porosity. Shrinkage showed no direct linear relationship with temperature, but lower shrinkage was observed for IR drying at high temperature compared to OV drying. Bulk density, final surface area, and final volume varied with drying conditions, with IR drying tending to preserve a larger surface area and volume. Thin-layer modelling revealed that the Weibull distribution best described the experimental drying curves for both methods and all temperatures, as evidenced by a high coefficient of determination and modelling efficiency, and low root mean square error and chi-square values. Correlation and ANOVA analyses indicated that under IR drying, several quality and physical parameters, including lightness, total colour difference, colour index, whiteness index, bulk density, final area, and final volume were significantly affected by drying temperature ($p< 0.0.05$), whereas under OV drying only bulk density and final area were significantly temperature dependent.

It is essential to mention that the analysis on effective moisture diffusivity and activation energy was not reported in our previously published study on red delicious apple slices due to the scope of the study objectives. In addition, the effect of diffusion path length on the initial, average and final half-thicknesses, predicted by Fick's equation, has not been clearly reported in the literature for the estimation of the effective moisture diffusivity and activation energy of different varieties of apple slices. Again, physical and thermal properties of agricultural products, such as mass and heat transfer, moisture distribution, and activation energy, are required for designing optimal drying equipment [24,32]. Activation energy is obtained by plotting the natural logarithm of the effective moisture diffusivity against the reciprocal of the absolute temperature [24]. By applying Fick's second law and treating the sample slices as infinite-thin slabs, the effective moisture diffusivity can be calculated [24]. According to Barforoosh et al. [24], the assumptions for isothermal conditions for both activation energy and effective moisture diffusivity calculations follows that the moisture is initially distributed evenly throughout the sample, mass transfer occurs uniformly toward the center, the surface moisture content of the sample reaches equilibrium with the ambient air, the surface resistance of the sample to mass transfer is significantly different from its internal resistance, mass transfer occurs solely by diffusion. All these assumptions align with the previously published study [27]. Therefore, the objective of the present study is to analyze the effect of drying temperatures and diffusion path lengths on effective moisture diffusivity and activation energy to further understand

 doi:10.20944/preprints202602.0791.v1

the governing mass transfer mechanisms and thermal sensitivity of the red delicious apple slices during convective drying.

2. Materials and Methods

2.1. Sample and Hot-Air Oven Drying Method

Fresh whole red delicious apples (Figure 1a) were purchased from a supermarket in Prague, Czech Republic. The samples were kept in a refrigerator at 5 °C. Before the experiments, the samples were removed and allowed to cool to a laboratory temperature of 24.26±0.50 °C and humidity of 41.6±2.42%. A slicer was used to cut the fresh apples into a cylindrical size of thickness of 8.07±0.05 mm and diameter of 66.27±3.13 mm (Figure 1b). The dimensions (diameter and thickness) of the fresh and dried apple sliced samples were accurately measured using a digital calliper with an accuracy of 0.01 mm. The weights of the fresh and dried apple sliced samples were measured using a digital balance with an accuracy of 0.01. The standard hot-air oven (MEMMERT UF55m GmbH + Co. KG, Buechenbach, Germany) was used for drying the thin-layer samples of the apple slices (Figure c) [27].

Figure 1. (a) Two fresh samples of whole red delicious apples, (b) thin-layer sample of the red delicious apple and (c) dried sample at 80 °C representing varying samples dried at 40, 50, 60 and 70 °C [27].

2.2. Dry Basis Moisture Content

The dry basis moisture content of the samples was calculated using equation (Equation (1)) [33–35].

$$M_t = \frac{(W_t - G)}{G} \quad (1)$$

where M_t is the dry basis moisture content of the sample at the moment of drying time t (g/g); W_t is the total mass of the sample (g) at the moment of drying time t, and G is the mass of dry matter (g).

2.3. Moisture Ratio

The moisture ratio was calculated using equation (Equation (2)) [33,35–38].

$$MR = \frac{(M_t - M_e)}{M_0 - M_e} \quad (2)$$

where MR is the moisture ratio (dimensionless), M_0 is the initial dry-basis moisture content (g/g), and M_e is the equilibrium moisture content (dry basis, often minimal and assumed negligible for many cases). The value of M_e can be neglected, as it is relatively small compared to the values of M_t and M_0. Therefore, (Equation (2)) can be rewritten in the form given in (Equation (3)) [17,19,33,36,39].

$$MR = \frac{M_t}{M_0} \quad (3)$$

 doi:10.20944/preprints202602.0791.v1

2.5. Shrinkage

The shrinkage (SK) was calculated as the percentage reduction in characteristic length from the initial state, $L_{i,}$ to the final state, L_f (Equation (4)), ensuring positive values for all drying conditions [40,41].

$$SK = \frac{L_i - L_f}{L_I} = 1 - \frac{L_f}{L_I} \quad (4)$$

2.6. Effective Moisture Diffusivity

In many drying processes, especially thin-layer drying, the moisture ratio (MR) follows Fick's second law (Equation (5)) [9,35,36,38,42].

$$MR = \frac{8}{\pi^2}\exp\left(-\frac{\pi^2 D_{eff} t}{4L^2}\right) \quad (5)$$

Taking logs of (Equation (6)) gives (Equation (7)) as follows:

$$\ln(MR) = ln\left(\frac{8}{\pi^2}\right) - \frac{\pi^2 D_{eff}}{4L^2} t \quad (6)$$

Plotting $ln(MR)$ versus time, the slope gives (Equation (5)) as follows:

$$D_{eff} = -\frac{4L^2 \times slope}{\pi^2} \quad (7)$$

where D_{eff} is the effective moisture diffusivity (m^2/s).

2.7. Activation Energy

Based on the diffusivity data at different drying temperatures, the Arrhenius equation can be fitted following equations (Equation (8) to Equation (10) [9,35,36,38,42].

$$D_{eff} = D_0 \exp\left(-\frac{E_a}{RT}\right) \quad (8)$$

Taking logs of (Equation (6)) gives (Equation (7)) as follows:

$$ln(D_{eff}) = ln(D_0) - \frac{E_a}{R}\left(\frac{1}{T}\right) \quad (9)$$

From a plot of $ln(D_{eff})$ versus 1/T, the slope gives (Equation (8)) as follows:

$$E_a = -(slope) \times R \quad (10)$$

where E_a is the activation energy (kJ/mol) and R = 8.314 J/mol·K

2.8. Descriptive Statistics

The experiments were repeated twice, and the data were presented as the means, standard deviation, and percentage coefficient of variation. The graphical illustrations were done using Statistica 13 software [43]. All the calculations were done using Microsoft Excel, version 2601 and verified by Python program inside a Jupyter Notebook using Anaconda Navigator.

3. Results and Discussion

3.1. Half-Thickness (L) of the Samples

In Fick's second law for slab-shaped materials such as thin-layer apple slices, the effective moisture diffusivity (Equation (7))) is related to the slope of the natural logarithm of the moisture ratio versus drying time. The half-thickness (L) of the sample directly affects the effective moisture diffusivity quadratically. The initial half-thickness, the final half-thickness and the average half-thickness of the samples were taken into consideration (Table 1) for the estimation of the effective moisture diffusivity and activation energy. The initial thickness represents the initial diffusion path for moisture before shrinkage starts. The final thickness represents the shortest diffusion path after maximum shrinkage. The average thickness represents an effective or average diffusion distance

 doi:10.20944/preprints202602.0791.v1

across the entire drying period. Kidane et al. [9] used the average thickness of 0.00525 m of apple slices yielding a half-thickness of 0.002625 in computing the effective moisture diffusivity. In this analysis, however, the initial, final, and average thickness, each with the corresponding half-thickness, were used to calculate the moisture diffusivity and the activation energy, which are discussed in the succeeding sections.

Table 1. Half-thickness of the samples at the initial, final and average.

T_{PR} (°C)	Test I			Test II		
	L_i (m)	L_f (m)	L_{avg} (m)	L_i (m)	L_f (m)	L_{avg} (m)
40	0.00375	0.00273	0.00324	0.003845	0.0025	0.0031725
50	0.003745	0.002195	0.00297	0.00393	0.002465	0.0031975
60	0.00415	0.00228	0.003215	0.00402	0.00247	0.003245
70	0.004065	0.002415	0.00324	0.004115	0.002275	0.003195
80	0.004095	0.002755	0.003425	0.004165	0.002465	0.003315

T_{PR}: Drying temperature; L_i: initial half-thickness; L_f: final half-thickness; and L_{avg}: average half-thickness.

3.2. Drying Curves at Varying Temperatures

3.2.1. Sample Weight Versus Drying Time

The change in sample weight with drying time at different drying temperatures between 40 and 80 °C of thin-layer red delicious apples for the duplicated experiments is shown in Figure 2. A decreasing trend was observed for all drying temperatures. At the onset of drying, the apple slices exhibited a rapid weight reduction, which can be attributed to the high rate of surface moisture evaporation. This period corresponds to the constant-rate drying phase, during which the rate of moisture removal is primarily governed by external mass transfer between the moist surface and the surrounding hot air. As drying progressed, the rate of weight loss gradually declined, indicating the transition into the falling-rate period, where internal diffusion of bound water becomes the limiting step. Higher drying temperatures resulted in a steeper decline in sample weight over time, confirming that increasing air temperature enhances the vapour pressure gradient and accelerates moisture removal. The final equilibrium weight was reached faster at higher temperatures due to the increased drying potential of the air and higher thermal energy available for water molecule migration [17,19,33,36,39].

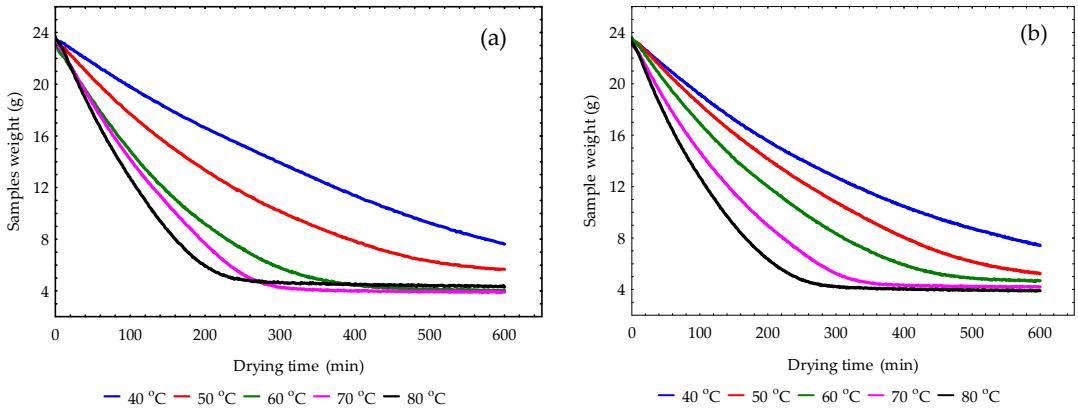

Figure 2. Sample weight versus drying time at varying drying temperatures for duplicated experiments (a) and (b) of thin-layer red delicious apple slices.

3.2.2. Moisture Content with Drying Time

The variation in moisture content (Equation (1).) with drying time at different drying temperatures between 40 and 80 °C for thin-layer red delicious apples in duplicated experiments is

 doi:10.20944/preprints202602.0791.v1

shown in Figure 3. The moisture curves followed a typical exponential decay pattern. Initially, the moisture content was high, and it decreased rapidly with time as free and loosely bound water were removed from the sample matrix. The drying rate then slowed considerably as the remaining moisture became more tightly bound to cellular structures such as polysaccharides, proteins and fibres. At elevated temperatures (≥ 60 °C), the drying curves became steeper, showing that the drying time required to reach a given moisture level decreased significantly. This reflects the increased moisture diffusivity at higher temperatures, as thermal energy reduces resistance to water transport within the tissue. Conversely, at lower temperatures, the drying curves (40 °C and 50 °C), the drying curves flattened out, indicating slower moisture migration and longer drying durations. These observations are consistent with Fickian diffusion behaviour, in which the effective moisture diffusivity increases exponentially with temperature following the Arrhenius relationship [8,36,44–46].

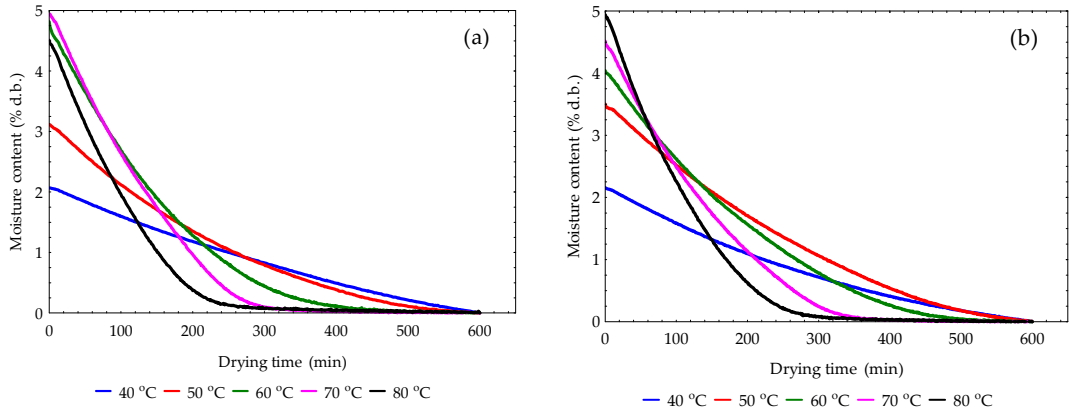

Figure 3. Moisture content versus drying time at varying drying temperatures for duplicated experiments (a) and (b) of thin-layer red delicious apple slices.

3.2.3. Moisture Ratio with Drying Time

The moisture ratio (MR) (Equation (3)) also showed an exponential decrease with drying time across all drying temperatures of thin-layer red delicious apples for the duplicated experiments, as shown in Figure 4. The MR-time curves at higher temperatures (60–80 °C) exhibited steeper slopes, reflecting faster moisture removal rates and shorter drying durations. The curves approached equilibrium more rapidly, indicating that the driving force for moisture diffusion, that is, the moisture concentration gradient, was much greater at elevated temperatures. At lower temperatures (40 and 50 °C), the curves declined more gradually, showing that the internal resistance to moisture migration dominated during the drying process. The slower diffusion behaviour corresponds to lower effective moisture diffusivity values, confirming that the drying process is controlled by internal moisture diffusion rather than surface evaporation during most of the falling-rate period. The shape of MR-time curves exhibited the characteristic single falling-rate period, with no distinct constant-rate region, typical of biological materials such as fruits and vegetables [1,9,19,36,44,45,47,48]. This behaviour suggests that diffusion is the governing mechanism throughout the drying process, and external mass transfer resistance is negligible [47]. Bai et al. [1] reported a similar moisture ratio of apple slices across different drying times and pretreatment methods. The authors indicated that with the extension of the drying time, the moisture ratio of the apple slices declined steadily. Kidane et al. [9] also studied the moisture ratio and time curves for apple slices in half-capacity and full-capacity solar dryers. They found that the moisture ratio decreased over time across all drying conditions, indicating the effectiveness of the drying process in reducing moisture content.

 doi:10.20944/preprints202602.0791.v1

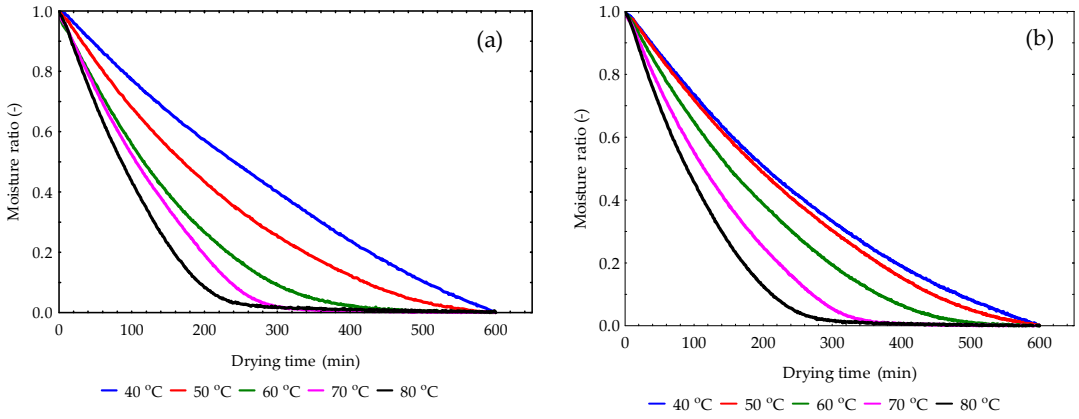

Figure 4. Moisture rate versus drying time at varying drying temperatures for duplicated experiments (a) and (b) of thin-layer red delicious apple slices.

3.3. Linear Fits and Effective Moisture Diffusivity of Varying Characteristic Lengths

The calculation of the effective moisture diffusivity D_{eff} by using Equation (7) requires not only the half-thickness of the sample, but also the slope from the linear relationship between the natural logarithm of the moisture ratio versus the drying time for the duplicated experiments shown in Figure 5. The determined slope values, coefficients of determination (R^2), and the D_{eff} for the varying characteristic lengths are presented in Table 2. The linear regression models showed a strong fit with R^2 values ranging from 0.9955 to 0.9971, confirming the suitability of Fick's second law to describe the falling rate period for drying samples of apple slices. In the falling rate period, the material surface is no longer saturated with water, and the drying rate is controlled by diffusion of moisture from the interior of solid to the surface [46,49]. The calculated D_{eff} values for the apple slices dried at temperatures between 40 and 80 °C ranged from 1.43×10^{-10} m²/s to 1.03×10^{-09} m²/s. D_{eff} values increased with drying temperatures. The increase in diffusivity with temperature is consistent with findings in drying kinetics studies [9,44,45,50,51]. The increase in drying temperatures accelerated the surface evaporation and enhanced the internal moisture movement. This trend indicates that water molecules within the apple matrix require less activation energy for diffusion at elevated temperatures due to increased vapour pressure, decreased viscosity, and enhanced mobility of bound water. The relationship between temperature and D_{eff} can be attributed to both physical and microstructural changes occurring in the tissue during drying, such as cell wall rupture and shrinkage, which facilitate internal moisture transport. The higher D_{eff} values at elevated temperatures imply a more rapid internal moisture migration rate, leading to shorter drying times. Conversely, lower temperatures yielded smaller D_{eff} values corresponding to slower moisture movement and longer drying durations [9,45].

It is important to highlight that for the duplicated tests conducted for the apple sample slices, the D_{eff} values calculated using the initial half-thickness were consistently the highest, followed by those obtained from the average half-thickness, while the final half-thickness produced the lowest values. This trend reflects the quadratic dependence of diffusivity on the characteristic length and the progressive shrinkage of the sample during drying. Using the initial thickness tends to overestimate D_{eff} because it assumes the diffusion path remains constant before shrinkage. The effective diffusion path shortens as the sample loses moisture and collapses structurally. The final thickness, on the other hand, tends to underestimate the D_{eff} since it represents only the geometry at the end of drying, when moisture has already reached equilibrium and diffusion nearly ceases. The average half-thickness therefore provides a balanced and physically realistic estimate that captures the mean diffusion distance throughout the process. The average characteristic length is preferred for diffusivity analysis in materials undergoing continuous shrinkage [9,45,47,48]. Kidane et al. [9] reported the D_{eff} values of apple slices ranging from 1.990×10^{-7} m²/s to 2.0599×10^{-7} m²/s under

 doi:10.20944/preprints202602.0791.v1

varying solar dryers, using the average thickness of the apple samples. Yilmaz et al. [44] also found D_{eff} values ranging from 6.81 × 10⁻¹⁰ m²/s to 3.27 × 10⁻⁸ m²/s for apricot dried under different pretreatments. Arulkumar et al. [45] also reported that D_{eff} values for paneer samples dried at 50 °C ranged from 2.15 × 10⁻⁸ to 2.40 × 10⁻⁸ m²/s. For samples dried at 55 °C, D_{eff} values ranged from 2.19 × 10⁻⁸ to 2.68 × 10⁻⁸ m²/s, and for 60 °C, D_{eff} values ranged from 3.61 × 10⁻⁸ to 3.85 × 10⁻⁸ m²/s. The values observed in this study in comparison with other works are under normal range of D_{eff} threshold of 10⁻⁸ to 10⁻¹² m²/s reported for food products [9,11,17,19,24,28,33,36,44,45,52].

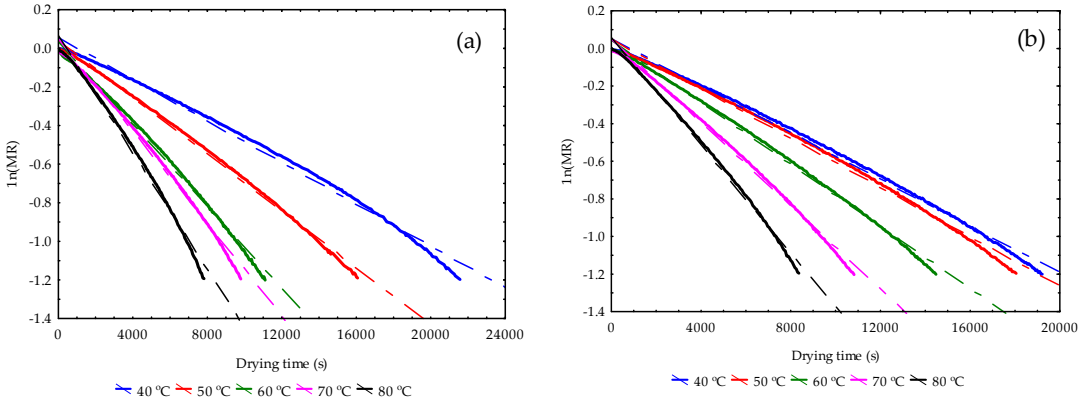

Figure 5. Linear fits of thin-layer samples under hot-air oven drying for (a) test I and (b) test II.

Table 2. Determined effective moisture diffusivity D_{eff} for varying characteristic lengths.

Tests	T_{PR} (°C)	Slope	R²	Initial length, L_i D_{eff} (m²/s)	Final length, L_f D_{eff} (m²/s)	Average length D_{eff} (m²/s)
I	40	–5.39963 × 10⁻⁰⁵	0.9932	3.07742 × 10⁻¹⁰	1.63098 × 10⁻¹⁰	2.29728 × 10⁻¹⁰
I	50	–7.33689 × 10⁻⁰⁵	0.9971	4.17038 × 10⁻¹⁰	1.43265 × 10⁻¹⁰	2.62292 × 10⁻¹⁰
I	60	–10.6852 × 10⁻⁰⁵	0.9959	7.45828 × 10⁻¹⁰	2.25119 × 10⁻¹⁰	4.47615 × 10⁻¹⁰
I	70	–11.9848 × 10⁻⁰⁵	0.9946	8.02625 × 10⁻¹⁰	2.83287 × 10⁻¹⁰	5.09896 × 10⁻¹⁰
I	80	–15.1687 × 10⁻⁰⁵	0.9930	10.309 × 10⁻¹⁰	4.66606 × 10⁻¹⁰	7.21155 × 10⁻¹⁰
II	40	–6.23954 × 10⁻⁰⁵	0.9964	3.73857 × 10⁻¹⁰	1.58049 × 10⁻¹⁰	2.54516 × 10⁻¹⁰
II	50	–6.59029 × 10⁻⁰⁵	0.9955	4.12524 × 10⁻¹⁰	1.62293 × 10⁻¹⁰	2.73077 × 10⁻¹⁰
II	60	–8.25406 × 10⁻⁰⁵	0.9973	5.40605 × 10⁻¹⁰	2.0409 × 10⁻¹⁰	3.52255 × 10⁻¹⁰
II	70	–11.0814 × 10⁻⁰⁵	0.9963	7.60492 × 10⁻¹⁰	2.32444 × 10⁻¹⁰	4.58455 × 10⁻¹⁰
II	80	–14.2947 × 10⁻⁰⁵	0.9959	10.05 × 10⁻¹⁰	3.52021 × 10⁻¹⁰	6.36652 × 10⁻¹⁰

T_{PR}: Temperature; D_{eff}: Effective moisture diffusivity and R²: Coefficient of determination.

 doi:10.20944/preprints202602.0791.v1

3.4. Shrinkage Behaviour of Apple Slices

Shrinkage is the reduction of volume and shape that cannot be neglected in drying problems [41,53]. The shrinkage values for the apple slices at varying drying temperatures ranging from 40 to 80 °C are presented in Table 3. Both tests demonstrated that apple slice thickness decreased significantly during drying, confirming that shrinkage is a direct consequence of moisture removal and structural collapse of the cellular matrix [1,15,54,55]. In test I, shrinkage increased from 27.2% at 40 °C to a maximum of 45.1% at 60 °C, then gradually declined to 32.7% at 80 °C. Similarly, in test II, shrinkage rose from 34.98% at 40 °C to 44.71% at 70 °C, and then slightly decreased to 40.82% at 80 °C. The mean shrinkage increased from 31.09% at 40 °C to a maximum of 42.65% at 70 °C, then slightly decreased to 36.77% at 80 °C. The lowest standard deviation of 2.91 was observed at 50 °C and 70 °C, indicating high repeatability and stable shrinkage behaviour. In contrast, the highest standard deviation values between 4.59 and 5.7, occurred at 40 °C and 80 °C, suggesting greater variability due to uneven moisture gradients. The percentage coefficient of variation values was below 18%, indicating good reproducibility of the results. However, these results suggest that shrinkage does not increase linearly with temperature but rather exhibits a peak around the mid-temperature range (60 to 70 °C), beyond which a slight reduction occurs. The shrinkage pattern with temperature suggests that while moderate heating promotes uniform moisture loss and structural softening, excessive heating may induce surface hardening, which restricts collapse and thus limits total thickness reduction. The variation in shrinkage peaks for tests I and II could be attributed to slight differences in sample uniformity or airflow conditions during the tests. Mayor and Sereno [15] and Hatamipour and Mowla [55] reported that fruit tissues exhibit maximum shrinkage at moderate temperatures due to the balance between internal vapour pressure and cell wall plasticity. Generally, in food systems, shrinkage is rarely negligible, and it's advisable to account for it when predicting moisture content profiles in the material undergoing dehydration. Loss of water and heating causes stress in the cellular structure of the food, leading to a change in shape and a decrease in dimension [15]. The relationship between shrinkage and the drying temperature is shown in Figure 6. A polynomial function suitably described the relationship with an R^2 of 0.985 compared to a linear model with an R^2 of 0.249.

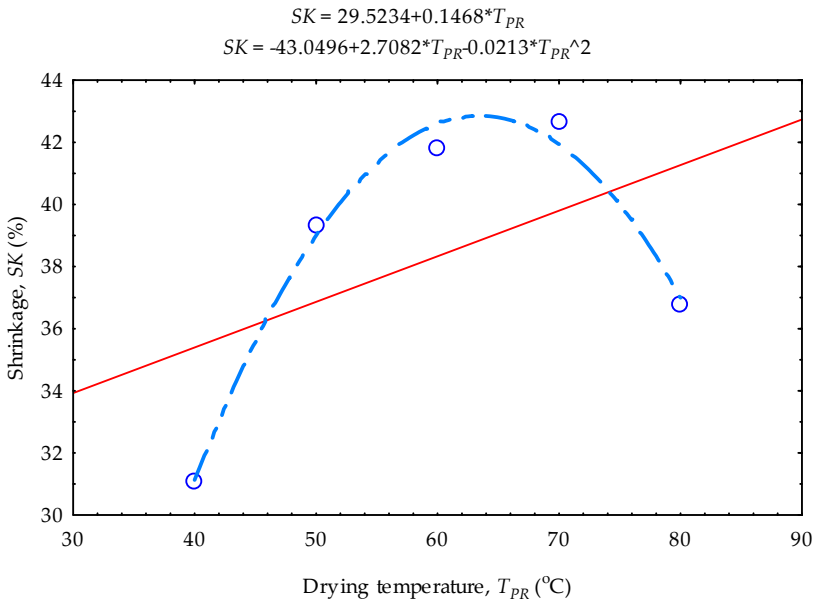

Figure 6. Shrinkage versus temperature dependence on samples of apple slices under hot air drying.

 doi:10.20944/preprints202602.0791.v1

Table 3. Shrinkage for apple slices under hot-air oven drying and their statistical metrics.

T_{PR} (°C)	Test I Shrinkage (%)	Test II Shrinkage (%)	Mean	SD	% CV
40	27.200	34.980	31.090	5.502	17.696
50	41.389	37.277	39.333	2.907	7.391
60	45.060	38.557	41.809	4.598	10.999
70	40.590	44.714	42.652	2.916	6.837
80	32.723	40.816	36.770	5.723	15.564

T_{PR}: Temperature; SD: Standard Deviation; CV: Coefficient of Variation.

3.5. Relationship Between Shrinkage and Effective Moisture Diffusivity

Shrinkage directly influences the D_{eff} by reducing the diffusion path length and altering the internal pore structure [15,41,53,54]. The observed 27–45% reduction in sample thickness implies a corresponding decrease in the diffusion distance, which would increase the apparent D_{eff} if not corrected for geometry. Therefore, accounting for shrinkage through the average half-thickness ensures that D_{eff} values represent the realistic, time-averaged internal transport behaviour. The results from both experimental tests confirm that ignoring shrinkage can lead to overestimation of the D_{eff}, particularly in the mid-temperature range where structural collapse is most severe. Both tests confirm that temperature strongly influences the magnitude and progression of shrinkage. Maximum deformation occurred between 60 and 70 °C, while shrinkage slightly declined at 80 °C due to case hardening and reduced flexibility of the surface [15,41,53–55].

3.6. Activation Energy forVarying Characteristic Lengths

The activation energy is the minimum energy required to initiate moisture diffusion or to break through the barrier and initiate the drying process [33,44,45]. The Arrhenius plots of natural logarithm of effective moisture diffusivity, D_{eff} versus the reciprocal of absolute temperature, $1/T_{PR}$ (K) for the two test conditions and three characteristic lengths are shown in Figure 7, and the determined activation energy, E_a values are given in Table 4. The coefficients of determination of the Arrhenius plots ranged from 0.8547 to 0.9622 for all the characteristic lengths and test conditions. At the upper end of $R^2 = 0.96$, the Arrhenius model fits the experimental data strongly suggesting that temperature has a dominant and predictable influence on D_{eff}. The linear behaviour confirms that moisture diffusion is primarily thermally activated, consistent with the physical meaning of activation energy [44,45]. At the lower end of $R^2 = 0.85$, there is still a strong relationship, but with slightly greater data scatter, indicating that other factors besides temperature, example, sample variability, shrinkage and/or moisture-dependent diffusivity may have influenced the results [41,53,54].

The E_a results ranged from 17.8290 to 28.3985 kJ/mol depending on the characteristic length and test condition. The E_a values were within the typical range between 6.80 and 78.93 kJ/mol reported for fruits, vegetables and other products [24,33,45–48,51,56–58], confirming the reliability of the obtained D_{eff} data. The computed E_a exhibited a clear dependence on the characteristic length used in the D_{eff} calculation. For test I, E_a decreased slightly from 28.40 kJ/mol (initial half-thickness) to 25.29 kJ/mol (final half-thickness) and then slightly increased to 27.12 kJ/mol (average half-thickness). For test II, the trend was similar but with lower magnitudes: E_a decreased from 23.67 kJ/mol (initial half-thickness) to 17.83 kJ/mol (final half-thickness) and increased again to 21.00 kJ/mol (average half-thickness). This variation reflects the role of sample shrinkage and geometry correction in defining the effective moisture transport mechanism [41,50,53,54]. Across all characteristic lengths, test I consistently produced higher activation energies than test II, with differences ranging from approximately 4.73 to 7.46 kJ/mol indicating that the samples of apple slices in test I required more energy for moisture migration, probably due to a higher initial moisture content or denser tissue structure, slight differences in air velocity or temperature uniformity, or variations in sample

 doi:10.20944/preprints202602.0791.v1

thickness or porosity that affected internal resistance to diffusion [41,50,53,54]. Therefore, lower values in test II suggest that the moisture transport process was somewhat easier likely because of structural softening or lower internal resistance during drying.

Furthermore, the initial half-thickness corresponds to the longest diffusion path, where moisture molecules required more energy to migrate through intact cell structure, leading to a higher E_a. As drying progresses and the sample shrinks, the reduced diffusion distance and partial cell wall rupture facilitate moisture transport, resulting in a lower E_a. At the final half-thickness, extensive shrinkage and microstructural collapse have occurred. The diffusion path is significantly shortened, and the porosity of the sample might have increased due to the formation of microcracks and voids during drying. These physical changes facilitate easier moisture movement, lowering the energy barrier for diffusion. Consequently, the activation energy is lowest at the final thickness [41,50,53,54]. Using the average half-thickness yields an intermediate activation energy that better reflects the overall diffusion process during drying, accounting for both structural collapse and moisture redistribution.

Finally, the mean activation energy varied between 21.56 and 26.03 kJ/mol across the different characteristic lengths. The standard deviation and the percentage coefficient of variation reflect the variability in the activation energy between the two tests. The initial half-thickness had the lowest standard deviation (SD = 3.34 kJ/mol) and coefficient of variation (CV = 12.84%) suggesting more consistent energy requirements early in drying when the geometry and structure were still uniform. The final thickness had the highest (SD = 5.28 kJ/mol) and (CV = 24.47%), indicating that diffusion energy was less stable, likely because structural deformation and porosity changes varied more strongly between tests. The average half-thickness showed moderate variability (SD = 4.00 kJ/mol) and (CV = 16.47%), indicating a balanced stability.

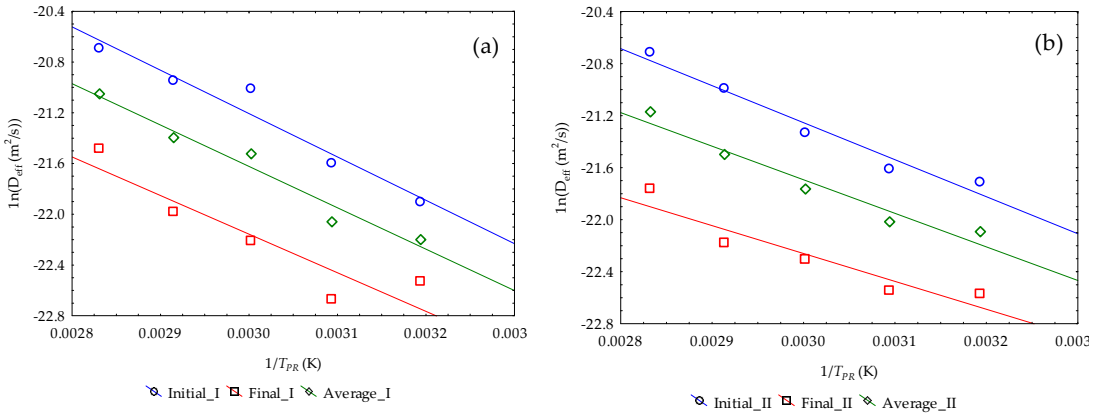

Figure 7. Arrhenius plot of the inverse of effective moisture diffusivity (D_{eff}) and inverse absolute temperature (T_{PR}) for varying characteristic lengths for (a) test I and (b) test II.

Table 4. Activation energy (E_a) for varying characteristic lengths and statistical metrics.

Characteristic length, L (m)	Test I E_a (kJ/mol)	Test II E_a (kJ/mol)	Mean	SD	% CV
Initial length	28.3985	23.6693	26.0339	3.3441	12.8450
R^2	0.9513	0.9616	0.9565	0.0073	0.7615
Final length	25.2899	17.8290	21.5594	5.2756	24.4701
R^2	0.8547	0.8855	0.8701	0.0218	2.5030
Average length	27.1197	21.4618	24.2907	4.0007	16.4701
R^2	0.9622	0.9478	0.9550	0.0102	1.0662

R^2: Coefficient of determination; SD: Standard Deviation and CV: Coefficient of Variation.

 doi:10.20944/preprints202602.0791.v1

3.7. Pre-Exponential Factor of the Arrhenius Equation

The pre-exponential factor D_0 is also termed as diffusion coefficient constant or Arrhenius factor [24,28]. The calculated D_0 values and their statistical metrics are presented in Table 5. The values ranged from 8.75×10^{-07} to 1.74×10^{-05} m²/s which were in the range of other agricultural products reported in the literature [24,28].

The results confirm that the Arrhenius relationship (Equation (6)) describing the temperature dependence of moisture diffusivity in the apple slices is physically realistic. The highest D_0 corresponds to the initial half-thickness, while the lowest D_0 occurs at the final half-thickness, indicating that the diffusion potential of the material decreases as drying progresses. Regarding the characteristic length on D_0, the initial half-thickness implies that the tissue structure at the start of drying is relatively open and retains more free water [41,53,54]. Water molecules have higher initial mobility, hence a greater theoretical diffusion potential. The higher D_0 reflects strong temperature sensitivity and the presence of loosely bound moisture. The final half-thickness implies that after prolonged drying, shrinkage and collapse of the cellular matrix reduce pore connectivity and moisture mobility. The decreased D_0 indicates that, even at an infinitely high temperature, moisture migration would remain limited due to structural resistance. The average half-thickness, which yields the intermediate D_0, represents a compromise between early-stage free water diffusion and late-stage bound moisture diffusion. This intermediate value best captures the effective diffusivity behaviour of the sample of the apple slices across the entire drying period. The coefficient of variation values for all characteristic lengths was high (>90%), indicating strong variability between the experimental tests results. It is worth nothing that the D_0 is derived from the intercept of the Arrhenius plot, which is highly sensitive to minor variations in diffusivity and temperature. In addition, biological materials like apple tissues are heterogeneous, with the differences in porosity, composition, and shrinkage behaviour that amplify the uncertainty of D_0 [41,53,54]. It is also essential to highlight the relationship between D_0 (Equation (8)) and the activation energy E_a (Equation (10)). The initial samples' characteristic length exhibited both high D_0 and high E_a, implying that diffusion is strongly temperature-dependent, that is, temperature changes produce significant variations in diffusivity. The final samples characteristic length had both low D_0 and high E_a reflecting sensitivity due to compacted structures and lower residual water content. The average samples' characteristic length maintained intermediate D_0 and E_a values, signifying balanced energy and mobility conditions that realistically describe the overall drying process.

Specifically, the pre-exponential factor (D_0) of the Arrhenius equation represents the theoretical diffusivity at infinite temperature or the maximum possible diffusivity of moisture within the material if there were no energy barrier to diffusion [9,45]. In drying of biological materials like apple slices, D_0 represents the intrinsic mobility of water molecules within the matrix, that is, how easily they could move if not limited by structural resistance or bonding energy. A higher D_0 means the material has more open pathways or higher inherent mobility, so even at low activation energies, diffusion occurs rapidly. A lower D_0 implies restricted molecular movement, often due to dense tissue, strong hydrogen bonding or limited pore connectivity [9,35,36,38,42].

Table 5. Determined parameters of the Arrhenius equation for varying characteristic lengths.

Tests	Characteristic length, L (m)	Pre-exponential factor D_0 (m²/s)	Mean	SD	% CV
I	Initial	1.74002×10^{-05}	1.0×10^{-05}	1.0×10^{-05}	99.69
II		3.01167×10^{-06}			
I	Final	2.19254×10^{-06}	1.0×10^{-06}	1.0×10^{-06}	125.14
II		1.33946×10^{-07}			
I	Average	7.23132×10^{-06}	1.0×10^{-06}	4.0×10^{-06}	126.41
II		8.7501×10^{-07}			

 doi:10.20944/preprints202602.0791.v1

3.8. Comparison of Experimental and Theoretical Effective Moisture Diffusivity

Using (Equation (11)), [9,35,36,38,42], the theoretical effective moisture diffusivity, $D_{eff_{th}}$ was computed and compared with the experimentally calculated D_{eff}. The results are presented in Table 6 and graphically shown in Figure 8 for the varying characteristic lengths and drying temperatures.

$$D_{eff_{th}} = D_0 \exp\left(-\frac{E_a}{RT}\right) \quad (11)$$

where $D_{eff_{th}}$ is the theoretical or predicted effective moisture diffusivity (m²/s).

Across all three characteristic lengths under both tests, the effective moisture diffusivity increased linearly with temperature. This reflects the expected Arrhenius-type relationship where the higher drying temperature accelerates internal moisture migration by increasing water molecule mobility and vapour pressure gradients. Both the experimental and predicted values showed the linear trend confirming that the Arrhenius model correctly captures the temperature dependence of diffusion [9,35,36,38,42]. The two experimental tests exhibited similar effective moisture diffusivity patterns indicating good repeatability of measurements. Average characteristic length produced the most representative of the effective moisture diffusivity estimates, accounting for both initial geometry and shrinkage during drying.

Table 6. Experimental and predicted effective moisture diffusivity D_{eff} for varying characteristic lengths and temperature.

Tests	Characteristic length	T_{PR} (°C)	D_{eff} (Experimental) (m²/s)	D_{eff} (Predicted) (m²/s)
I	Initial	40	3.07742×10^{-10}	3.1872×10^{-10}
I		50	4.17038×10^{-10}	4.46686×10^{-10}
I		60	7.45828×10^{-10}	6.13471×10^{-10}
I		70	8.02625×10^{-10}	8.27095×10^{-10}
I		80	1.0309×10^{-09}	1.0964×10^{-09}
I	Final	40	1.63098×10^{-10}	1.3254×10^{-10}
I		50	1.43265×10^{-10}	1.79017×10^{-10}
I		60	2.25119×10^{-10}	2.37467×10^{-10}
I		70	2.83287×10^{-10}	3.09856×10^{-10}
I		80	4.66606×10^{-10}	3.98266×10^{-10}
I	Average	40	2.29728×10^{-10}	2.16466×10^{-10}
I		50	2.62292×10^{-10}	2.98801×10^{-10}
I		60	4.47615×10^{-10}	4.04547×10^{-10}
I		70	5.09896×10^{-10}	5.3813×10^{-10}
I		80	7.21155×10^{-10}	7.04348×10^{-10}
II	Initial	40	3.73857×10^{-10}	3.39266×10^{-10}
II		50	4.12524×10^{-10}	4.49491×10^{-10}
II		60	5.40605×10^{-10}	5.85554×10^{-10}
II		70	7.60492×10^{-10}	7.51137×10^{-10}
II		80	1.005×10^{-09}	9.5005×10^{-10}
II	Final	40	1.58049×10^{-10}	1.42191×10^{-10}
II		50	1.62293×10^{-10}	1.75754×10^{-10}
II		60	2.0409×10^{-10}	2.14493×10^{-10}
II		70	2.32444×10^{-10}	2.58749×10^{-10}
II		80	3.52021×10^{-10}	3.08839×10^{-10}
II	Average	40	2.54516×10^{-10}	2.3013×10^{-10}
II		50	2.73077×10^{-10}	2.97002×10^{-10}
II		60	3.52255×10^{-10}	3.7748×10^{-10}
II		70	4.58455×10^{-10}	4.73107×10^{-10}
II		80	6.36652×10^{-10}	5.85425×10^{-10}

 doi:10.20944/preprints202602.0791.v1

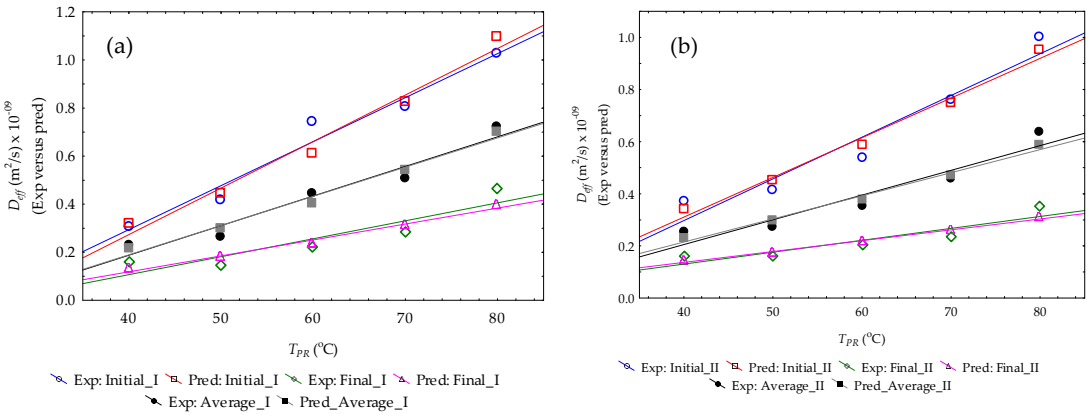

Figure 8. Experimental and predicted effective moisture diffusivity (D_{eff}) against temperature for varying characteristic length for (a) test I and (b) test II.

The statistical performance indicators obtained from the comparison between the experimental and predicted effective moisture diffusivity using all temperatures and replicate data combined (ten data points) for each characteristic length are presented in Table 7. Compared with single-temperature (two-data point) evaluations, the combined analysis provides a statistically robust approach. It is therefore the preferred basis for interpreting the temperature dependence of moisture diffusivity in red delicious apple slices. In addition, the high R^2 values (0.89–0.97), which match the model efficiency (EF) values confirm that the Arrhenius model fits the experimental diffusivity data well over the temperature range (40–80 °C), indicating that the Arrhenius model explains more than 89% of the observed variation in D_{eff}. The RMSE and MAE values are on the order of 10^{-11} m²/s, which are negligible compared to diffusivities of the order 10^{-10} m²/s. MAPE < 12% indicates the average relative error between experimental and predicted diffusivities is small confirming model reliability. The mean absolute percentage error (% Error) between the experimental and predicted diffusivities ranged from 0.29 to1.38% indicating efficient model accuracy. However, the negative bias values (–0.29 to –1.38%) observed before absolute transformation suggest a slight underprediction trend, particularly at the final characteristic length.

Besides, among the three characteristic lengths, the average length yielded the highest coefficient of determination (R^2 = 0.97) and the lower error values, indicating that it provides the most realistic representation of the actual diffusion path length during drying. This result implies that the mean structural dimension accounts for both the initial tissue geometry and subsequent shrinkage effects, thereby yielding more accurate diffusivity estimation. The initial length (R^2 = 0.95) also showed strong correlation and low deviation, representing the diffusion behaviour before significant structural deformation. In contrast, the final length yielded a slightly lower correlation (R^2 = 0.89) and the highest MAPE (12%) attributed to the increased structural collapse, internal resistance, and porosity changes that typically occur during the final drying stage.

Table 7. Statistical metrics between experimental and predicted effective moisture diffusivity D_{eff}.

Characteristic lengths	R^2	RMSE	MAE	MAPE	EF	% Error
Initial	0.951	5.58×10^{-11}	4.44×10^{-11}	7.105	0.951	0.293
Average	0.965	3.01×10^{-11}	2.77×10^{-11}	7.393	0.965	0.487
Final	0.886	3.29×10^{-11}	2.83×10^{-11}	12.021	0.886	1.385

R^2: Coefficient of determination, RMSE: Root Mean Square Error, MAE: Mean Absolute Error, MAPE: Mean Absolute Percentage Error and EF: Model Efficiency.

 doi:10.20944/preprints202602.0791.v1

5. Conclusions

The drying curves of thin-layer samples of red delicious apples (sample weight versus time, moisture content versus time and moisture ratio versus time) were described to estimate the effective moisture diffusivity and activation energy at temperatures ranging from 40 to 80 °C. The final equilibrium weight was reached faster at higher temperatures due to the increased drying potential of the air and higher thermal energy available for water molecule migration. Again, at elevated temperatures ≥ 60 °C, the drying curves became steeper, showing that the drying time required to reach a given moisture level decreased significantly. In contrast, at temperatures ≤ 50 °C, the drying curves flattened, indicating slower moisture migration and longer drying times. The determined negative slope values from the linear relationship between the natural logarithm of the moisture ratio versus drying time for varying characteristic lengths showed a strong fit with R^2 values ranging from 0.9955 to 0.9971, confirming the suitability of Fick's second law to describe the falling rate period of drying of agricultural products such as apples. The calculated effective moisture diffusivity values for the apple slices dried at varying temperatures between 40 and 80 °C ranged from 1.43×10^{-10} m^2/s to 1.03×10^{-09} m^2/s. The effective moisture diffusivity increases linearly with temperature across all characteristic lengths, and that the average characteristic length provided the most representative measure of internal mass-transfer resistance. The mean activation energy varied between 21.56 and 26.03 kJ/mol across the different characteristic lengths. However, using the average half-thickness yielded an intermediate activation energy that better reflects the overall diffusion process, accounting for both structural collapse and moisture redistribution. The pre-exponential factor values of the Arrhenius model ranged from 1.34×10^{-10} m^2/s to 8.75×10^{-10} m^2/s across all characteristic lengths. Based on these values, the theoretical effective moisture diffusivities across all characteristic lengths were calculated, ranging from 1.33×10^{-10} m^2/s to 1.10×10^{-09} m^2/s. Both the experimental and predicted values showed a linear trend, confirming that the Arrhenius model correctly captures the temperature dependence of diffusion. The high R^2 values being equal to high modelling efficiency, and very low root mean square error and mean absolute error) validated the reliability, accuracy and physical consistency of the Arrhenius-based model for predicting the effective moisture diffusivity in apple slices across the drying temperature range studied. Future analysis of this study will focus on the infrared drying of the red delicious apple slices based on similar characteristic lengths and drying temperatures to complete the overall analysis of the previously published study on the investigation of the effects of infrared and hot-air oven drying methods on drying behaviour and colour parameters of red delicious apple slices.

Author Contributions: Conceptualization. O.D., A.K., Č.M. and D.H.; Methodology. O.D., A.K., Č.M. and A.S.; Validation. O.D., A.K., Č.M., A.S. and D.H.; Formal analysis. O.D., A.K., Č.M., A.S. and D.H.; Data curation. O.D., A.K.; Č.M. and A.S.; Writing—original draft. O.D., A.K. and Č.M.; Writing—review and editing. O.D., A.K., Č.M. and D.H. All authors have read and agreed to the published version of the manuscript.

Funding: The study was supported by the Internal Grant Agency of Czech University of Life Sciences Prague, Grant Number: IGA Project Number – 2024:31130/1312/3108.

Institutional Review Board Statement: Not applicable.

Informed Consent Statement: Not applicable.

Data Availability Statement: The data presented in this study are available upon request from the corresponding author.

Conflicts of Interest: The authors declare no conflict of interest.

 doi:10.20944/preprints202602.0791.v1

References

1. Bai, J-W.; Zhang, L.; Aheto, J.H.; Cai, J-R.; Sun, L.; Tian, X-Y. Effects of different pretreatment methods on drying kinetics, three-dimensional deformation, quality characteristics and microstructure of dried apple slices. Innovative Food Science and Emerging Technologies. 2023, 83, 103216.
2. Joardder, M.U.H.; Karim, M.A. Drying kinetics and properties evolution of apple slices under convective and intermittent-MW drying. Thermal Science and Engineering Progress. 2022, 30, 101279.
3. Joardder, M.U.H.; Karim, A.; Kumar, C. Effect of temperature distribution on predicting quality of microwave dehydrated food. J. Mechan. Eng. Sci. 2013, 5, 562–568.
4. Orsat, V.; Yang, W.; Changrue, V.; Raghavan, G.S.V. Microwave-assisted drying of biomaterials. Food Bioprod. Process. 2007, 85(3), 255–263.
5. Amanor-Atiemoh, R.; Zhou, C.; Wahia, H.; Mustapha, A. T.; Zhou, R. Acoustically-aided osmo-dehydration pretreatments under pulsed vacuum dryer for apple slices: Drying kinetics, thermodynamics, and quality attributes. Journal of Food Science. 2020, 85(11), 3909–3919.
6. Kaleta, A.; Gornicki, K.; Winiczenko, R.; Chojnacka, A. Evaluation of drying models of apple (var. Ligol) dried in a fluidized bed dryer. Energy Conversion and Management. 2013, 67, 179–185.
7. Baysal, T.; Ozbalta, N.; Gokbulut, S.; Capar, B.; Gurlek, G. Investigation of effects of various drying methods on the quality characteristics of apple slices and energy efficiency. Journal of Thermal Science and Technology. 2015, 35(1), 135–144.
8. Alibas, I. Microwave, air and combined microwave–air-drying parameters of pumpkin slices. LWT-Food Sci. Technol. 2007, 40(8), 1445–1451.
9. Kidane, H.; Farkas, I.; Buzas, J. Performance evaluation of solar drying chambers and drying kinetics of apple slices. Energy Reports. 2025a, 13, 4528–4540.
10. Kidane, H.; Farkas, I.; Buzas, J. Mathematical modelling of golden apple drying and performance evaluation of solar drying systems using energy and exergy approach. Scientific Reports. 2025b, 15(7805), 1–16.
11. Chen, C.; Venkitasamy, C.; Zhang, W.; Khir, R.; Upadhyaya, S.; Pan, Z. Effective moisture diffusivity and drying simulation of walnuts under hot air. International Journal of Heat and Mass Transfer, 2020, 150, 119283.
12. Rabha, D.K.; Muthukumar, P. Performance studies on a forced convection solar dryer integrated with a paraffin wax-based latent heat storage system. Sol. Energy. 2017, 149, 214–226.
13. Mujumdar, A.S. Research and development in drying: recent trends and future prospects. Dry. Technol., 2004, 22, 1–26.
14. Zhang, W.; Pan, Z.; Xiao, H.; Zheng, Z.; Chen, C.; Gao, Z. Pulsed vacuum drying (PVD) technology improves drying efficiency and quality of Poria cubes. Dry. Technol., 2018, 36(8), 908–921.
15. Mayor, L.; Sereno, A.M. Modelling shrinkage during convective drying of food materials: a review. J. Food Eng., 2004, 61, 373–386.
16. Karathanos, V.T.; Villalobos, G.; Saravacos, G.D. Comparison of two methods of estimation of the effective moisture diffusivity from drying data. J. Foods Sci., 1990, 55(1), 218–231.
17. Ning, Z.; Khir, R.; Niederholzer, F.; Pan, Z. Characteristics of moisture diffusivity and shrinkage evolution of in-hull almonds under hot air drying. LWT–Food Science and Technology, 2025, 232, 118455.
18. Rafiee, S.; Sharifi, M.; Keyhani, A.; Omid, M.; Jafari, A.; Mohtasebi, S.S.; Mobli, H. Modeling effective moisture diffusivity of orange slice (Thompson CV.). Int. J. Food Prop., 2010, 13, 32–40.
19. Kayran, S.; Doymaz, I. Infrared drying and effective moisture diffusivity of apricot halves: influence of pretreatment sand infrared power. J. Food Process. Preserv. 2017, 41, 1–8.
20. Crank, J. The mathematics of diffusion. Oxford University Press, Inc (1975).
21. Akhijani, H.S.; Abrahosseini, A.; Kianmehr, M.H. Effective moisture diffusivity during hot air solar drying of tomato slices. Res. Agric. Eng., 2016, 62(1), 15–23.
22. Babalis, S.J.; Belessiontis, V.G. Influence of the drying conditions on the drying constants and moisture diffusivity during the thin-layer drying of figs. J. Food Eng., 2004, 65, 449–458.
23. Kumar, R.; Sharma, A.K.; Agnihotri, K. Dynamics of an innovation diffusion model with time delay. East Asian J. Appl. Math. 2017, 7(3), 455 –481.

 doi:10.20944/preprints202602.0791.v1

24. Barforoosh, M.Y.; Borghaee, A.M.; Rafiee, S.; Minaei, S.M.; Beheshti, B. Determining the effective diffusivity coefficient and activation energy in thin-layer drying of Haj Kazemi peach slices and modeling drying kinetics using ANFIS. International Journal of Low-Carbon Technologies. 2024, 19, 192–206.
25. Younas, S.; Arqam, U.; Wang, X.; Liu, C.; Huang, Y.; Feng, L. Ultrasound-assisted controlled ice-seeding during freezing: Impact on quality attributes, freeze drying kinetics, structural modification, supercooling suppression and moisture mobility of apple. Food Control. 2026, 181, 111761.
26. Subrahmanyam, K.; Gul, K.; Paridala, S.; Sehrawat, R.; More, K.S.; Dwivedi, M.; Jaddu, G. Effect of cold plasma pretreatment on drying kinetics and quality attributes of apple slices in refractance window drying. Innovative Food Science and Emerging Technologies. 2024, 92, 103594.
27. Dajbych, O.; Kabutey, A.; Mizera, Č.; Herák, D. Investigation of the effects of infrared and hot air oven drying methods on drying behaviour and colour parameters of red delicious apple slices. Process, 2023, 11, 3027.
28. Pinheiro, M.N.C.; Castro, L.M.M.N. Effective moisture diffusivity prediction in two Portuguese fruit cultivars (Bravo de Esmolfe apple and Madeira banana) using drying kinetics data. Heliyon. 2023, 9(7), e17741.
29. Pinheiro, M.N.C.; Madaleno, R.O.; Castro, L.M.M.N. Drying kinetics of two fruits Portugues cultivars (Bravo de Esmolfe apple and Madeira banana): An experimental study. Heliyon. 2022, 8(4), e09341.
30. Chen, A.; Achkar, G.E.L.; Liu, B.; Bennacer, R. Experimental study on moisture kinetics and microstructure evolution in apples during high power microwave drying process. Journal of Food Engineering. 2021, 292, 110362.
31. Bi, J.; Yang, A.; Liu, X.; Wu, X.; Chen, X.; Wang, Q.; Lv, J.; Wang, X. Effects of pretreatments on explosion puffing drying kinetics of apple chips. LWT–Food Science and Technology. 2015, 60(2), 1136–1142.
32. Mujumdar, A.S. Handbook of Industrial Drying, 3rd ed. Taylor & Francis Group CRC, Boca Raton, 2006.
33. Khater, E-S.G.; Bahnasawy, A.H.; Elwakeel, A.E.; Tantawy, A.A.; Elbeltagi, A.; Salem, A.; Marey, S.A.; Okasha, A.M.; Metwally, K.A. Comparative analysis of drying kinetics, thermodynamic properties, and mathematical modeling of pomegranate peel (Punica granatum L.) in a hybrid solar dryer and an oven dryer. Scientific Reports. 2025, 15(26288, 1–25.
34. Wang, H.; Liu, Z.-L.; Vidyarthi, S.K.; Wang, Q.-H.; Gao, L.; Li, B.-R.; Wei, Q.; Liu, Y.-H.; Xiao, H.-W. Effects of different drying methods on drying kinetics, physicochemical properties, microstructure, and energy consumption of potato (*Solanum tuberosum* L.) cubes. *Dry. Technol.* **2021**, *39*, 418–431.
35. Xie, Y.; Lin, Y.; Li, X.; Yang, H.; Han, J.; Shang, C.; Li, A.; Xiao, H.; Lu, F. Peanut drying: Effects of various drying methods on drying kinetic models, physicochemical properties, germination characteristics, and microstructure. *Inf. Process. Agric.* **2022**.
36. Komolafe, C.A.; Ojediran, J.O.; Ajao, F.O.; Dada, O.A.; Afolabi, Y.T.; Oluwaleye, I.O.; Alake, A.S. Modelling of moisture diffusivity during solar drying of locust beans with thermal storage material under forced and natural convection mode. Case Studies in Thermal Engineering. 2019, 15, 100542.
37. Dina, S.F.; Ambarita, H.; Napitupulu, F.H.; Kawai, H. Study on effectiveness of continuous solar dryer integrated with desiccant thermal storage for drying cocoa beans. Case Studies in Thermal Engineering. 2015, 5, 32–40.
38. Xiao, H.W.; Pang, C.L.; Wang, L.H.; Bai, J.W.; Yang, W.X.; Gao, Z.J. Drying kinetics and quality of Monukka Seedless grapes dried in an air–impingement jet dryer. *Biosyst. Eng.* **2010**, *105*, 233–240.
39. Zhang, J.; Karim, A.; Sutar, P.P.; Mujumdar, A.S.; Wang, Z-X.; Shi, Y-S.; Liu, S-L.; Lv, W-Q.; Xiao, H-W. Sustainable development of drying technologies for agricultural products: recent advances, challenges, and future prospects. Renewable and Sustainable Energy Reviews. 2026, 226, 116419.
40. Li, C.; Ren, G.; Zhang, L.; Duan, X.; Wang, Z.; Ren, X.; Chu, Q.; He, T. Effects of different drying methods on the drying characteristics and drying quality of *Cistanche deserticola*. LWT-Food Sci. Technol. 2023, 184, 115000.
41. Mugi, V.R.; Chandramohan, V. Shrinkage, effective diffusion coefficient, surface transfer coefficients and their factors during solar drying of food products – A review. Solar Energy. 2021, 229, 84–101.
42. Gilago, M.C.; Mugi, V.R.; Chandramohan, V.P. Evaluation of drying kinetics of carrot and thermal characteristics of natural and forced convection indirect solar dryer. Results Eng. 2023. 18, 101196.

 doi:10.20944/preprints202602.0791.v1

43. Statsoft Inc. *STATISTICA for Windows*; Statsoft Inc.: Tulsa, OK, USA, 2013.
44. Yilmaz, M.S.; Sakiyan, O.; Isci, A. Effect of different pretreatments on drying characteristics and physicochemical properties of apricot (*Prunus armeniaca* L.). Journa of Food Process Engineering. 2024, 47, e14757.
45. Arulkumar, M.; Pandian, N.K.S.; Murugan, B.; Nambi, V.E.; Sivaranjani, S.; Baskaran, D.; Pugazhenthi, T.R.; Kishore, S.G.; Pandiselvam, R. Drying kinetics, effective moisture diffusivity and activation energy of osmotic pretreated hot-air-dried paneer cubes. Journal of Food Processing and Preservation. 2023, 1–17.
46. Akpinar, E.K. Mathematical modelling of thin layer drying process under open sun of some aromatic plants. Journal of Food Engineering. 2006, 77(4), 864–870.
47. Doymaz, I. Convective air drying characteristics of thin layer carrots. Journal of Food Engineering. 2004, 61, 359–364.
48. Madamba, P.S.; Driscoll, R.H.; Buckle, K.A. The thin-layer drying characteristics of garlic slices. Journal of Food Engineering. 1996, 29, 75–97.
49. Diamante, L.M.; Munro, P.A. Mathematical modelling of thin layer solar drying of sweet potato slices. *Solar Energy*. 1993,51, 271–276.
50. Ramakrishnan, S.R.; Chelliah, R.; Antony, U.; Oh, D-H. Characterization of drying kinetics and moisture diffusivity in finger millet using fluidized bed drying. Journal of Stored Products Research. 2025, 113, 102700.
51. Cavalcanti-Mata, M.E.; Duarte, M.E.; Tolentino, M.; Mendes, F.A.; Batista, L.; de Lima, J.M.; Lucio, A.; Nascimento, A.P.; Almeida, R.D.; Lisboa, H.M. Drying kinetics of industrial pineapple waste: effective diffusivity and thermodynamics properties resulting from new mathematical models derived from the Fick equation. Processes, 2024, 12(6), 1198.
52. Zogzas, N.; Maroulis, Z.; Marinos-Kouris, D. Moisture diffusivity data compilation in foodstuffs. Dry. Technol. 1996, 14(10), 2225–2253.
53. Koua, B.K.; Koffi, P.M.E.; Gbaha, P. Evolution of shrinkage, real density, porosity, heat and mass transfer coefficients during indirect solar drying of cocoa beans. J. Saudi Soc. Agric. Sci. 2019, 18, 72–82.
54. Li, L.; Zhang, M.; Zhou, L. A promising pulse-spouted microwave freeze drying method used for Chinese yam cubes dehydration: Quality, energy consumption, and uniformity. Drying Technology. 2019, 148–161.
55. Hatamipour, M.S.; Mowla, D. Shrinkage of carrots during drying in an inert medium fluidized bed. Journal of Food Engineering. 2002, 55(3), 247–252.
56. Waheed, M.A.; Komolafe, C.A. Temperatures dependent drying kinetics of cocoa beans varieties in air-ventilated oven. Frontiers in Heat and Mass Transfer. 2018, 12(8), 1–7.
57. Tulek, Y. Drying kinetics of oyster mushroom (Pleurotus ostreatus) in a convective hot air dryer. J. Agr. Sci. Techn. 2011, 13, 655 –664.
58. Mirzaee, E.; Rafiee, S.; Keyhani, A.; Emam-Djomeh, Z. Determining of moisture diffusivity and activation energy in drying of apricots. Res. Agric. Eng. 2009, 55, 114–120.
59. Li, C.; Ren, G.; Zhang, L.; Duan, X.; Wang, Z.; Ren, X.; Chu, Q.; He, T. Effect of different drying methods on the drying characteristics and drying quality of *Cistanche deserticola*. LWT–Food Sci. Technol. 2007, 184, 115000.
60. Komolafe, C.A.; Oluwaleye, I.O.; Adejumo, A.O.D.; Waheed, M.A.; Kuye, S.I. Determination of moisture diffusivity and activation energy in the convective drying of fish. International Journal of Heat and Technology. 2018, 36(4), 1262–1267.
61. Mujumdar, A.S. Handbook of industrial drying. 3rd ed. Taylor and Francis Group CRC, Boca Raton, 2006.